ARTICLES

Characteristic Length of Dynamic Glass Transition near T_g for a Wide Assortment of Glass-Forming Substances

E. Hempel,[†] G. Hempel,[†] A. Hensel,[‡] C. Schick,[‡] and E. Donth*[,†]

Fachbereich Physik, Universität Halle, D-06099 Halle (Saale), Germany, and Fachbereich Physik, Universität Rostock, D-18051 Rostock, Germany

Received: April 6, 1999; In Final Form: December 8, 1999

Dynamic heterogeneity is an active field of glass-transition research. The length scale of this heterogeneity is called the characteristic length. It can be calculated from complex heat capacity curves in the equilibrium liquid or from dynamic calorimetry curves corrected with regard to nonequilibrium. No molecular parameters or microscopic models are necessary for obtaining the length. We report the characteristic length near glass temperature for about 30 glass formers including small-molecule liquids, polymers, silicate glasses, a metallic glass, a liquid crystal, and a plastic crystal. The lengths are between 1.0 and 3.5 nm with certain cumulations between 1.0 and 2.0 nm and between 2.5 and 3.5 nm. To try a correlation to other properties, we find that at least two should be included, e.g., Angell's fragility and the distance of T_g from the crossover temperature, T_c.

Introduction

The characteristic length ξ_α of glass transition corresponds to the size of cooperatively rearranging regions CRR of Adam and Gibbs,[1] $V_\alpha = \xi_\alpha^3$. This length, or at least an indication for dynamical heterogeneity, has been tried to be extracted from such diverse techniques as NMR,[2−4] atomic force microscopy,[5] calorimetry,[6,7] dielectric relaxation[8,9] on polymers and molecular liquids confined within nanoporous glass or confined within mobile amorphous layers between crystal lamellas,[10] confined thin film liquids under shear,[11] probe molecule rotational/translational differences,[12,13] dynamic and static light scattering,[14−17] nonresonant spectral hole burning,[18] and molecular dynamics simulations.[19,20] A detailed review is written by Sillescu.[21] The present consensus is that the length is approximately 1−5 nm.

The spatial aspect of dynamic heterogeneity, if any, is an abstract picture of how we can imagine a fluctuating space−time pattern of different mobilities across the sample. In two simple versions, the sample is partitioned into small ($<\xi_\alpha$) partial systems whose dynamic properties are characterized by a local frequency[22] or by a local relaxation time.[23] The parameters of such a picture are the mobility differences between the partial systems ($\delta \ln \omega$ as extracted from the width of a susceptibility peak, e.g., from $\epsilon''(\ln \omega)$ or $c_p''(\ln \omega)$), a decision between islands of mobility[24] or clusters of immobility,[25] and the characteristic length of glass transition being a length scale of the mobility pattern.

A powerful experimental method for the elucidation of dynamic heterogeneity could be dynamic neutron (or X-ray) scattering. Unfortunately, the present time window on the nanometer scale[26,27] is too short to reach such slow dynamics that is expected to have a dynamic heterogeneity, i.e., below the crossover region of glass transition.

Of course, there must also be some reflection of the mobility pattern by the structure, even by the static structure factor. The effect, however, is expected to be *very* small[28] since the free volume regulating the relation between mobility and structure is only a very small fraction of the total volume. Scattering experiments did not yet find any indication for such a length in the structure factor.[29]

The only method that delivers an explicit formula for the characteristic length is from calorimetry.[6,30] All parameters needed can be unambiguously calculated from dynamic calorimetry (Section 3, below). The formula (see eq 1, below) is from thermodynamic fluctuation theory, applied to the dynamic glass transition, and no molecular estimations or microscopic models are necessary for obtaining the length. Using heat capacity spectroscopy[31,32] over a relatively wide temperature and frequency range, we can also get temperature dependencies of ξ_α for such samples that have a good adhesion to the substrate and the nickel layer of the 3ω apparatus.[33]

The derivation of eq 1 from the fluctuation dissipation theorem FDT is in detail published elsewhere,[6,28,30,34−36] so that only four short comments will be made. (i) The dimension of eq 1 is a volume, and the expected order of a few nanometers is always obtained from this formula. (ii) The amplitude of thermodynamic fluctuation depends strongly on the size of the subsystem to be considered. Equation 1 answers the question about that subsystem size whose fluctuations are determined via the FDT by linear response across the glass transition. (iii) The subsystem defined by eq 1 is the CRR. This definition is a consequence of the verbal Adam Gibbs CRR definition by

* Corresponding author. Fax: ++49 345 55 27 017. E-mail: donth@physik.uni-halle.de.
[†] Universität Halle.
[‡] Universität Rostock.

10.1021/jp991153f CCC: $19.00
Published on Web 02/25/2000

TABLE 1: Summary of the Investigated Substances

				DSC				TMDSC				
no.	substance, abbreviation	M_0, g/mol	fullname	T_g, °C	δT, K	Δc_p, J/g K	$\xi_\alpha(T_g)$, nm	T_ω (t_p/s), °C	δT, K	Δc_p, J/g K	$\xi_\alpha(T_\omega)$, nm	rem.
1	PMMA	100	poly(methyl methacrylate)	95	5.1	0.25	1.5	97.5 (60)	8.5	0.23	1.1	*e, g*
2	PEMA	114	poly(ethyl methacrylate)	70	3.8	0.26	1.8	75.5 (60)	7.5	0.22	1.1	*g*
3	PPrMA	128	poly(*n*-propyl methacrylate)	51	4.8	0.20	1.4	56.5 (60)	10.0	0.18	0.9	*g*
4	P*n*BMA	142	poly(*n*-butyl methacrylate)	25	5.4	0.19	1.2	32.5 (60)	8.0	0.16	0.9	*g*
5	P*n*PenMA	156	poly(*n*-pentyl methacrylate)	7	7.0	0.29	1.0	8.5 (60)	11.3	0.20	0.8	*g*
6	P*n*HMA	170	poly(*n*-hexyl methacrylate)	−20	8.8	0.29	1.0	−12 (60)	12.1	0.33	0.9	*g*
7	BIBE	268	benzoin isobutyl ether	−52	2.1	0.49	3.2	−48.5 (60)	2.8	0.49	2.7	
8	AMPEK	196	poly(ether ketone) from ICI	153	2.0	0.25	3.2	153 (600)	2.2	0.24	3.0	*a, g*
9	PS	104	poly(styrene) PS168N BASF	100	2.3	0.28	3.0	103.5 (60)	3.4	0.28	2.5	*a, g*
10	PVAC	86	poly(vinyl acetate)	40	2.3	0.44	3.2	45.5 (24)	3.6	0.39	2.3	*b, g*
11	CKN	126	$40Ca(NO_3)_2$ $60KNO_3$	64	2.4	0.55	3.2	68.5 (60)	2.9	0.46	2.6	*b, g*
12	$Na_2O{\cdot}SiO_2$	91	natrium disilicate	458	8.0	0.27	1.8	470 (750)	12.1	0.28	1.4	*b, g*
13	DGG	59	standard glass 1 from DGG[45]	538	12.1	0.25	1.4	576 (120)	14.0	0.23	1.3	*b, g*
14	$2SN_4$	954	liquid sulfur bridged twin crystal[45]	78	2.5	0.45	1.1	84 (100)	2.7	0.42	1.1	*b, g*
15	SBR1500	61	styrene−butadiene−rubber, 23% styrene	−58	2.4	0.46	2.7	−56 (60)	3.2	0.45	2.2	*g*
16	P(*n*BMA-stat-S) 2%S	141	poly(*n*-butyl methacrylate-*stat*-styrene) 2% styrene	30	4.3	0.22	1.5	34.5 (48)	10.7	0.22	0.9	*a, f, g*
17	$Zr_{65}A_{17.5}Cu_{17.5}Ni_{10}$	78	metallic glass	373	6.3	0.24	2.6	389 (60)	13.4	0.18	1.6	*d, h*
18	MAG	65	mixed alkali glass	477	10.8	0.22	1.5					*c*,[52] *i*
19	glycerol	92		−84	2.5	1.02	2.9	−80 (60)	2.6	0.97	2.6	*i*
20	salol	214	phenyl salicylate	−54	1.8	0.53	3.1	−51 (60)	2.3	0.55	3.3	*h*
21	OTP	230	*o*-terphenyl	−24	2.3	0.46	3.0					*c, i*
22	sorbitol	182	D(−) sorbitol	−12	2.0	1.04	3.6					*c, i*
23	BMPC	296	bis(methoxy phenyl)cyclohexane	−31	2.1	0.41	3.0	−26.5 (60)	2.5	0.36	3.1	*h*
24	selenium	79		37	2.7	0.38	3.0					*c*,[53] *i*
25	PVC	62	poly(vinyl chloride)	80	2.4	0.31	3.1					*c*,[44] *i*
26	silicate glasses	30...58		476−545	17.6 ± 5.3	0.27 ± 0.05	1.2					*c*,[54] *i*
27	cyclohexanol	100	phase I (ODIC)	−124	2.0	0.26	2.4					c,[55] *i*
28	B_2O_3	70	bortrioxid	274	8.1	0.50	1.5	305 (60)	12.5	0.61	1.3	*i*

[a] TMDSC from ref 45. [b] DSC + TMDSC from ref 45. [c] No TMDSC, DSC partly from literature. [d] Determination of fragility m was difficult because the Vogel temperature T_∞ could not be estimated for this metallic glass. We obtained m values between 80 and 160 depending on T_∞ and used $m = 120$. A m value ≥ 80 at T_g seems certain. [e] Commercial sample with plasticizer. A systematic paper on the poly(methacrylate) series with comparable samples is in preparation.[56] [f] Fragility from dielectric WLF parameters[49] is smaller ($m \approx 70$). [g] Fragility m from a modified Narayanaswamy Moynihan procedure with current reference temperature.[43] [h] Ditto but with a fixed reference and Vogel temperature. [i] Fragility m from ref 51.

statistical independence of fluctuations from the environment, and of the assumption[37,38] that for freely fluctuating subsystems inside a large total system both temperature and entropy can simultaneously fluctuate, and that these subsystem fluctuations are independent[37] from the conditions for the total system (V = const, or p = const, or $\delta Q = 0$, or others) as long as the latter is much larger than the subsystem. (iv) The CRR is related to the Fourier components of slow molecular motion in the dispersion zone of dynamic glass transition ("functional subsystem[35] for the α relaxation"). Possible subsystem interrelations in other frequency zones or even on the basis of the Gibbs distribution are not relevant. The dynamic heterogeneity can therefore disengage from structure, and the characteristic length can strongly[33] depend on the temperature.

The aim of this paper is to report on a systematic study of characteristic lengths ξ_α at the glass temperature T_g (from DSC) and up to 30 K above T_g (from temperature-modulated DSC = TMDSC) for a wide assortment of glass formers. Furthermore, we try to find correlations of ξ_α with Angell's fragility parameter[39] and with the distance of the crossover temperature from T_g.

Experimental Section

The acronyms and numbers of the substances used are listed in Table 1. The molecular mass of what is used as a "particle" for the calculation of a "cooperativity" N_α is also given: N_α is the number of such particles in one average CRR with volume V_α.

A DSC 7 apparatus (Perkin-Elmer) was used for a cooling−heating cycle between far above and far below the glass temperature T_g with rates of $|dT/dt| = 10$ K/min. The sample masses were about 10 mg; the equilibration time far above T_g was 10 min. T_g was calculated by an equal-area construction of the heating curve using tangents from far below and far above T_g.

The advantage of isothermal TMDSC would be that after long equilibration time the experiment is for the equilibrium state of the sample. We would not have nonequilibrium problems that must be corrected, as for DSC. The disadvantage would be that large time intervals are needed in comparison with DSC. We used a compromise, a TMDSC measurement (also with the Perkin-Elmer apparatus) using a small underlying cooling rate with sawtooth modulation so that the temperature during one period (standard period $t_p = 60$ s, temperature amplitude $T_a = 0.2$ K) is practically constant ($\Delta T \lesssim 0.5$ K).

Evaluation Methods. The evaluation of the DSC and TMDSC data was aimed at getting reliable parameters Δc_p, $\bar{c}_p$, and δT for our thermodynamic fluctuation formula

$$V_\alpha = \xi_\alpha^3 = k_B T^2 \Delta(1/c_V)/\rho \delta T^2 \quad (1)$$

$$N_\alpha = V_\alpha \rho / M_0 \quad (2)$$

$$\Delta(1/c_V) = (1/c_V)^{\text{glass}} - (1/c_V)^{\text{liquid}} \approx (\Delta 1/c_p) \approx (\Delta c_p/\bar{c}_p^2)(1 + (1/4)(\Delta c_p/\bar{c}_p)^2 + ...) \quad (3)$$

where c_p and c_V are specific heats (J/g K) at constant pressure and volume, respectively, ρ is the mass density (g/cm^3), and $\delta T^2 \equiv (\delta T)^2$ is the mean-square temperature fluctuation of one average CRR, functional[35] to the dynamic glass transition (K^2).

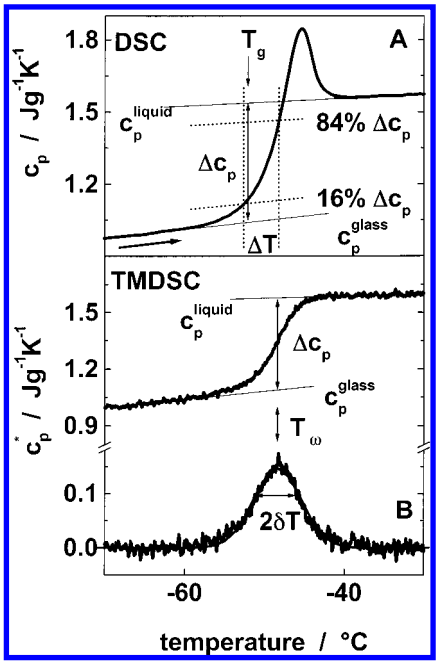

Figure 1. Scheme for the determination of the quantities needed for the characteristic length from DSC (A) and TMDSC (B) experiments for the BIBE example, 7 from Table 1. (A) T_g is calculated by an equal area construction; c_p^{liquid} and c_p^{glass} are tangents in the liquid and glass temperature ranges on the c_p curve, respectively. (B) T_ω is the peak maximum temperature from Gaussian fit for c_p''. δT is the temperature dispersion.

For TMDSC, the amounts of Δc_p, $\bar{c}_p$, and δT were determined from isochronal (ω = const) runs (Figure 1). The peak of the imaginary part, $c_p''(T, \omega = \text{const})$, is approximated by a Gauss curve

$$c_p''(T) = \text{const} \cdot \exp\left(-(T - T_\omega)^2/2\delta T^2\right) \tag{4}$$

that determines δT as the dispersion of this approximation. The relation between this dispersion and the mean temperature fluctuation of a CRR is analyzed in the Appendix. The heat capacity step Δc_p is determined at the c_p'' maximum temperature T_ω for the frequency ω applied ($\omega = 2\pi\nu = 2\pi/t_p$). Tangent constructions are used to determine c_p^{glass} and c_p^{liquid} at $T = T_\omega$, and $\bar{c}_p = (c_p^{glass} + c_p^{liquid})/2$.

Equation 3 contains two approximations: $c_p \approx c_V$, and a Taylor series to use Δc_p. In ref 40 we find Δc_V and Δc_p values for 4 small-molecule glass formers and 14 polymers. We calculated the correction factor from these data as

$$S \equiv \Delta(1/c_V)/\Delta(1/c_p) = 0.74 \pm 0.22 \tag{5}$$

where ± 0.22 is the standard deviation (the extreme S values are 1.07 and 0.26). All N_α values from our isobaric experiments in Figures 3 and 4 are corrected by $S = 0.74$, the ξ_α values by $S^{1/3}$. The corresponding expected uncertainty of the length ξ_α is about 9%.

For DSC, the correction of partial freezing-in is made by a modified Narayanaswamy Moynihan (MNM) procedure[41−43] to get traces equivalent to $c_p'(T)$ curves in the equilibrium. The parameters δT and T_g are determined from the heating curve, and Δc_p, c_p^{glass}, c_p^{liquid}, and $\bar{c}_p$ were then determined analogously to Figure 1, but directly from the DSC curves at T_g.

The δT parameter was calculated from the β parameter of the Kohlrausch function used in the MNM procedure for the underlying equilibrium retardation function

$$\phi = 1 - \exp(-(t/\tau)^\beta) \tag{6}$$

$$\beta\, \delta \ln \omega = 1 \tag{7}$$

$$\delta T/\delta \ln \omega = dT/d \ln \omega|_{WLF}^{T_g} \tag{8}$$

Equation 7 defines an equivalent mobility width $\delta \ln \omega$ of the imaginary part of a susceptibility, $\chi''(\ln \omega)$, when calculated by numerical Fourier transformation from the Kohlrausch function. An equivalent Gauss function on $\ln \omega$, pinned at the half-maximum values, would, instead of the 1 in eq 7, give values between 1.04 and 1.12, weakly increasing with β. Equation 8 is the local time−temperature superposition principle, connecting the dispersions on the left-hand side with the slope of the α relaxation trace in a $T-\ln \omega$ diagram, on the right-hand side, when fitted, e.g., by a WLF equation. Our MNM procedure delivers this slope. We calculated also the fragility parameter m at T_g from this slope

$$m = (\mathrm{d} \log_{10} \omega/\mathrm{d} \ln T)_{T_g} \tag{9}$$

The values obtained correspond to literature values (see some examples in Table 2). In the last column of Table 1 the source of the fragility m used in the figures is remarked.

For substances (Se, PVC, ..., labeled by *c* and reference in Table 1) whose DSC traces are taken from literature, we used the following "rules of thumb" for an estimation of δT[30,44]

$$\delta T = \Delta T/2.5 \quad \text{for heating} \tag{10}$$

$$\delta T = \Delta T/4.0 \quad \text{for cooling} \tag{11}$$

with ΔT the temperature interval where the $c_p(T)$ curve from DSC varies between 16% and 84% of the Δc_p step. These rules are checked for several substances where the full MNM procedure was applied or both DSC and TMDSC curves are available.

The accuracy of the characteristic lengths is estimated to be within 85% and 125% of the ξ_α values given in Figures 3 and 4, which correspond to the estimate that the V_α and N_α values are accurate within a factor of ~2 (50...200%). The main sources of the partial uncertainties were the experimental verification of a Gauss fit for isochronal $c_p''(T)$ curves—the uncertainty of δT is then about 10%—(Figure 1), the uncertainty of eqs 10 and 11 (about 10...20%), the uncertainty of the tangent construction for determining Δc_p (10%) and $\bar{c}_p$ (5%), in particular for curved glass and liquid traces, the uncertainty of the KWW-to-Gauss transformation eq 7, the physical uncertainty of the MNM procedure (20%), and the unknown concrete value of S according to eq 3.5 for the c_p/c_V conversion (30%).

TABLE 2: Comparison of Fragilities *m* from the Modified Narayanaswamy Moynihan Procedure[43] of DSC-Heating Run with the Fragilities from Literature[57] Using Dielectric (ϵ), Calorimetric (C_p), Viscoelastic Shear Compliance (J), and Quasielastic Light-Scattering Experiments (Φ)

substance	*m* from DSC	*m* from ref 57	method(s)[57]
PMMA	160	145	$J(t)$
PS	127	139	$J(t)$
CKN	112	93	$\Phi(t)$, $C_p(\omega)$
PVAC	95	95	$J(t)$
salol	64	73	$\Phi(t)$, $C_p(\omega)$, $\epsilon(\omega)$
glycerol	47	53	$C_p(\omega)$, $\epsilon(\omega)$

Results and Discussion

The glass temperatures, T_g, the average temperature fluctuations of one CRR from DSC, $\delta T(T_g)$, and the characteristic

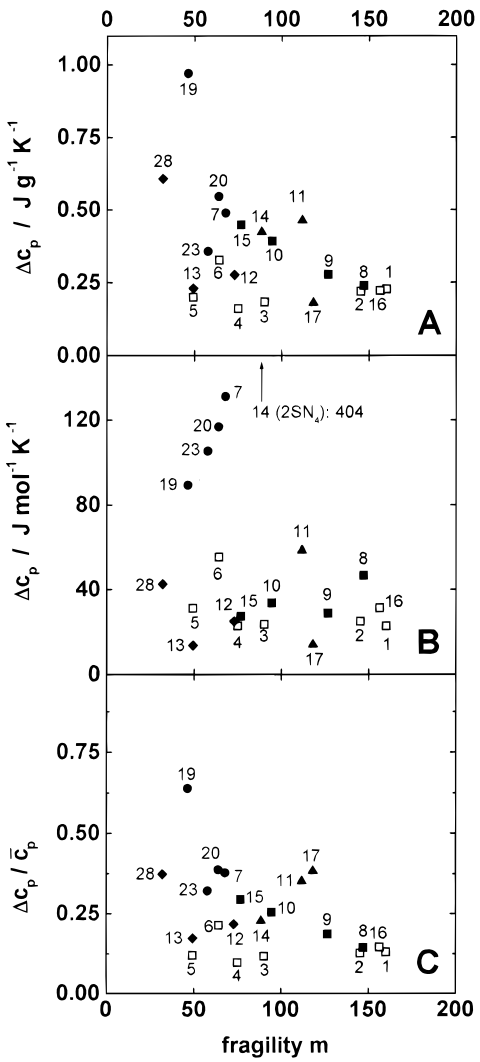

Figure 2. Dependence of the absolute specific (Δc_p) (A), molar (B), and relative step height ($\Delta c_p/\bar{c}_p$) (C) of heat capacity at $T = T_\omega$ on the fragility m (from TMDSC). Open symbols: P*n*AMA series. Solid symbols are for the other classes: polymers (■), silicate and related inorganic glasses (◆), small-molecule organic glass formers (●), and others (▲). The labels correspond to the numbers in Table 1.

lengths, $\xi_\alpha(T_g)$, are listed in Table 1 above, ditto the "dynamic" glass temperatures T_ω (ω = angular frequency), the associated $\delta T(T_\omega)$, and $\xi_\alpha(T_\omega)$ values from TMDSC. It should be mentioned again that the DSC and TMDSC experiments are independent measurements. As expected,[33] $T_\omega > T_g$, $\delta T(T_\omega) > \delta T(T_g)$, and $\xi_\alpha(T_\omega) < \xi_\alpha(T_g)$ in the frame of experimental uncertainty. The frequency associated with T_g from DSC can approximately be calculated from[32,45]

$$\omega \approx 5.5\dot{T}/\delta T(T_g) \qquad (12)$$

A theory for the factor 5.5 in eq 12 will be published elsewhere. The heat capacity steps from TMDSC, Δc_p and $\Delta c_p/\bar{c}_p$, do not strictly correlate with the fragility m (Figure 2). It seems, unexpectedly, that the larger specific and relative Δc_p values are observed for the smaller m. Probably[46] the correlation could be improved by dividing or uniting the M_0 particles to appropriate "beads". This method, however, has inevitably a certain residual arbitrariness and was not used here.

Instead we divided our substance set into four classes with different symbols: polymers (■, □), silicate and related inorganic glasses (◆), small-molecule organic glass formers (●),

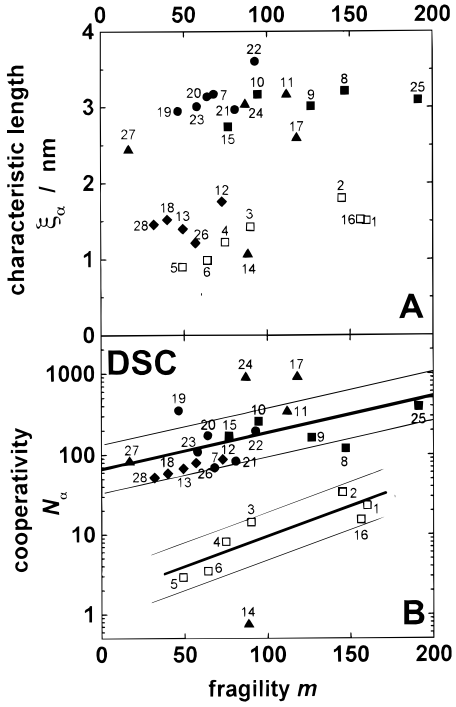

Figure 3. Dependence of the characteristic length ξ_α of glass transition at T_g (A) and of the cooperativity N_α at T_g (B) on the fragility m (from DSC). Open symbols: P*n*AMA series. Solid symbols: the others as defined in Figure 2. The labels correspond to the numbers in Table 1. Additional straight lines for linear fits including the 95% confidence interval (independently estimated) are indicated for both sets.

and the others (▲): a salt melt (11), a large LC molecule (14), a metallic glass (17), selenium (24), and a plastic crystal (27).

The characteristic lengths ξ_α and the cooperativities N_α at T_g according to eqs 1 and 2 do also not strictly correlate with the fragility (Figure 3). We observe two cumulations of the ξ_α values around $\xi_\alpha = 1.5$ nm and $\xi_\alpha = 3.0$ nm, with a significant gap between 2.0 and 2.5 nm. The N_α values show, cum grano salis, certain correlations. We have two sets for N_α, partly different from the ξ_α cumulations.

(i) The group of poly(*n*-alkyl methacrylates), P*n*AMA (□). The labels 1, 2, ..., 6 are the number of C atoms in the *n*-alkyl side chain. The trend is that N_α increases with decreasing C number and increasing fragility m. The trend goes far beyond what is expected from the increasing molecular mass of the monomeric units.

(ii) The other substances (■, ◆, ●, ▲) show a tendency that N_α increases with m, but there are clear exceptions outside the data uncertainty: 14 = the large twin liquid crystal, 19 = glycerol, 24 = selenium, and 17 = the metallic glass.

The $N_\alpha(m)$ correlations for the two sets are different. In the polymethacrylate group P*n*AMA (i) decreasing fragility m and increasing C number of the side group are associated with a shift of the crossover frequency from about megahertz for the methyl member, PMMA, to about 2 Hz for the hexyl member, P*n*HMA.[47] This corresponds to a shift of about 1 frequency decade per C unit. In the other substances (ii), the crossover frequency is, as a rule, in the megahertz-to-gigahertz range, and mostly unknown.

In total, we expect to get a better correlation with two parameters when the crossover parameters for all substances will be known: the fragility parameter m and a distance parameter between the crossover frequency and the glass frequency, or, in other words, between the crossover temperature T_c and the glass temperature T_g.

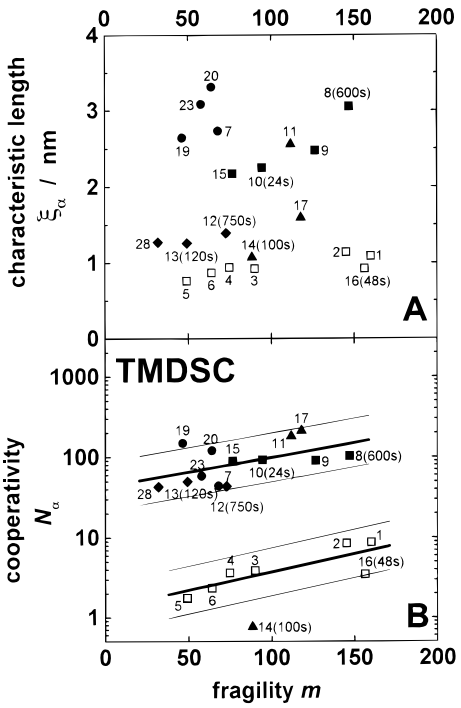

Figure 4. Dependence of the characteristic length ξ_α of glass transition for $t_p = 60$ s (A) and the cooperativity N_α (B) on the fragility m (from TMDSC). Open symbols: P*n*AMA series. Solid symbols: the others as defined at Figure 2. The labels correspond to the numbers in Table 1. Periods $t_p \neq 60$ s are indicated in parentheses. Additional straight lines for linear fits including the 95% confidence interval (independently estimated) are indicated for both sets.

The N_α and ξ_α values from TMDSC show a similar picture (Figure 4). The ξ_α and N_α values are smaller, as mentioned above, the ξ_α cumulations are not so sharp but still significant, and the difference in the slopes of the two $N_\alpha - m$ correlations is smaller than for the DSC correlations in Figure 3.

We think that the ξ_α cumulation reflects, via a general[33] temperature dependence, the possibility of different cage[43,48] size for the high-temperature process above the crossover temperature.

Let us mention again that the characteristic volume V_α and the characteristic length ξ_α follow directly from eq 1, without any microscopic model, whereas the cooperativity N_α, a particle number (eq 2), needs the definition of what a particle with M_0 is. We always choosed a whole molecule or, for polymers, a monomeric unit for a particle. Such particles are the units for an independent particle diffusion or for a Rouse diffusion, respectively. For the few examples so far investigated above the crossover temperature T_c we observed $N_a \approx 1$ for the *a* process.[32,47,49] The *a* process, above T_c, is described via mode-coupling theory[48] by a molecular cage of next neighbors. The $N_a \approx 1$ value corresponds to the size of a "cage door" for escaping of the molecule from the *a* process cage. The α process, below T_c, is discussed[43] as cage escaping assisted by a cooperativity shell. $N_\alpha \approx 1$ thus corresponds to missing of the cooperativity shell near and above the crossover for the scenario I.[50] The diffusion aspect of dynamic glass transition does not allow division of the particles into beads.

Let us finally discuss the characteristic lengths, ξ_α, and the steps in heat capacity, Δc_p, with respect to the number of parameters they depend on. We call a factual dependence on one single parameter (e.g., on the fragility) "similarity", and the dependence on two or more parameters "individuality".[28] This terminology stems from geometry: two triangles are similar if they are distinct only in size, one parameter; different size and angles make individual triangles, two or three parameters. On the other hand, "congruence" would correspond to phase-transition universality, not observed for glass transition.

Our Figures 2−4 show clearly that ξ_α and Δc_p reflect "individuality" of the glass transition. The lengths between 1 and 3.5 nm are small in comparison with typical lengths of thermodynamic transitions. Although the reduced Arrhenius diagram shows "similar" curves (Angell plot[51]), the liquid structure of the components is multifarious (compare, e.g., the liquid structures of PVAC and the metallic glass). It seems that this multifariousness shines through to the glass transition in the length range of 1−3.5 nm generating the "individuality" scatter of the Δc_p and ξ_α data when plotted against the fragility parameter m.

Once again: it seems one of the most important quests for the glass transition is why, despite the multifariousness of structures, the glass transition in different substances has a "similar" dynamic scenario. Our results indicate an intermediate stage. The length scale of 1−3.5 nm reflects a weakened multifariousness as an "individuality". The Δc_p step is obviously organized in regions of this size.

Conclusion

Calorimetric experiments on a wide assortment of molecular glass formers confirm that the characteristic length of glass transition near T_g is typically 1.0−3.5 nm. It seems that at least two parameters are needed for a correlation with other glass-transition properties: The characteristic length is affected by individual properties of the molecules.

Acknowledgment. We thank Dr. S. Kahle (now at IFK Jülich) and Dr. R. Unger for their help with the data evaluation. We thank the Deutsche Forschungsgemeinschaft DFG (Sonderforschungsbereich 418) and the Fonds Chemische Industrie FCI for financial support. The first who observed the ξ_α cumulation was Dr. K. Schröter, Halle.

Appendix

In general, the temperature fluctuation of subsystems is at present not directly accessible by experiments. Periodic calorimetry yields entropy fluctuations. Temperature fluctuations, however, can be calculated from entropy fluctuations using the formulas of linear response and the fluctuation dissipation theorem FDT. Such calculations are simplified when the central part of the calorimetric loss peak can be approximated by a Gauss function, eq 4 of the text.

The Appendix is to show that, modeling the imaginary part of heat capacity $C''(T)$ by a Gauss function with dispersion δT, the average temperature fluctuation of a CRR is equal to this δT, if temperature and entropy are considered as a conjugate pair (heat) in linear response and if time−temperature superposition eq 8 is locally linear, i.e., $dT/d \ln \omega = \text{const}$ across the dispersion zone.

Consider heat $dQ = T\,dS$ with a dynamic entropy compliance

$$J_S^* \equiv (1/T)\, c_p^* = (1/T)\,(c_p' - ic_p'') \tag{A1}$$

and a dynamic temperature modulus

$$G_T^* = G_T' + iG_T'' \tag{A2}$$

Linear response implies that for the same state

$$J_S^*(\omega)G_T^*(\omega) = 1 = \text{real} \tag{A3}$$

The average temperature fluctuation of a CRR, $\overline{\Delta T^2}$, is the integral over the spectral density of temperature fluctuation, $\Delta T^2(\omega)$

$$\overline{\Delta T^2} = 2\int_0^\infty \Delta T^2(\omega)\, d\omega \tag{A4}$$

The fluctuation dissipation theorem FDT for entropy and for temperature connects the spectral densities with the imaginary parts of corresponding susceptibilities

$$\Delta T^2(\omega) = k_B T\, G_T''(\omega)/\pi\omega \tag{A5}$$

$$\Delta S^2(\omega) = k_B T\, J_S''(\omega)/\pi\omega \tag{A6}$$

Neglect the influence of any work term in the internal energy. The integral of eq A5 over the dispersion zone of dynamic glass transition then gives

$$\overline{\Delta T^2} = RT^2\Delta(1/c)/N_\alpha M_0 \tag{A7}$$

This is the thermodynamically one-dimensional variant of our eqs 1 and 2 of the main text with no index at the specific heat capacity c. Further, $R = N_A k_B$, and the molar mass defines the particles.

We also need the Kramers Kronig relation for the calculation of $c'(\omega)$ from $c''(\omega)$

$$c'(\omega) = \frac{1}{\pi}\int_{-\infty}^{\infty}\frac{c''(\omega')\, d\omega'}{\omega' - \omega} + c^{\text{glass}} \equiv H(c'') + c^{\text{glass}} \tag{A8}$$

where the Hilbert transform H is a Cauchy principal value integral and $c''(-\omega) \equiv c''(\omega)$. The map from the T domain to the ln ω domain for the Gauss function eq 4 is

$$c''(\omega) = \frac{1}{2}\sqrt{\frac{\pi}{2}}\frac{\Delta c}{\delta \ln \omega}\exp\left(-\frac{\ln^2(\omega/\omega_T)}{2(\delta \ln \omega)^2}\right) \tag{A9}$$

with δ ln ω the dispersion of this logarithmic Gauss function, ω_T the frequency of its maximum, and the linear relation

$$dT/d \ln \omega = \delta T/\delta \ln \omega \tag{A10}$$

ω_T corresponds to T_ω in eq 4. The $c'(\ln \omega)$ and $c''(\ln \omega)$ curves are represented for a set of δ ln ω parameters in Figure 5. For $\delta \ln \omega \lesssim 2$, we find nonrealistic overshoots in c' (as typical for resonances), and for large $\delta \ln \omega > 3$ values the c' curve tends to an error integral, $1 - \phi(y)$ with $y = \ln \omega$. Typical values are $dT/d \log_{10} \omega = 3$ K/decade and $\delta T = 2.5$ K as for fragile polymers. Then $\delta \ln \omega = (2.5 \ln 10)/3 \approx 1.9$ corresponds to about $\beta \approx 1/\delta \ln \omega \approx 0.52$. This means that the Gauss function can only be a certain approximation for the central part of the C'' peak, when overshoots will be completely avoided as for retardation.

Our aim is the calculation of a correction factor

$$F(\delta \ln \omega, \gamma) \equiv \overline{\Delta T^2}/\delta T^2 \tag{A11}$$

correcting δT^2 from the $c''(T)$ dispersion to get $\overline{\Delta T^2}$ as an average CRR temperature fluctuation upon the condition that N_α should be the same for δT^2 from eqs 1 and 2 with $c_p = c_V$

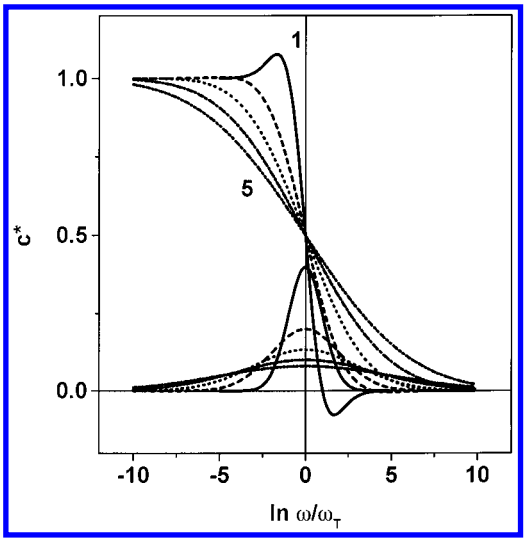

Figure 5. Real and imaginary part for a logarithmic Gauss function, i.e., for c^* as a function of $\ln(\omega/\omega_T)$ for five given values of δ ln ω (δ ln ω = 1, 2, 3, 4, 5); see text. ω_T is the maximum position of the imaginary part.

and $\overline{\Delta T^2}$ from eq A7. We introduce the symbols γ and $\tilde{c}^*$ for

$$\gamma = \Delta c/c^{\text{glass}} \quad \text{and} \quad \tilde{c}^* = c^*/\Delta c \tag{A12}$$

Then, from eqs A1−A10, we obtain

$$F = \frac{2}{\pi\Delta c\Delta(1/c)}\, Im\int_{-\infty}^{\infty}\frac{d \ln \omega}{\tilde{c}^*(\omega)} \tag{A13}$$

Unfortunately we could not find as yet an analytical[58] solution of eq A13 for the Gauss function. The numerical solution of the integral in

$$F(\delta \ln \omega, \gamma) = \frac{2}{\pi}(1+\gamma)\int_{\ln \omega=-\infty}^{\infty}\frac{\tilde{c}''\, d(\ln \omega)}{[\gamma H(\tilde{c}'') + 1]^2 + \gamma^2\tilde{c}''^2} \tag{A14}$$

gives

$$F(\delta \ln \omega, \gamma) = 1.00 \pm 0.01 \tag{A15}$$

for the logarithmic Gauss function in the γ range from $0.05 \le \gamma \le 0.5$ and a δ ln ω range from $1 \le \delta \ln \omega \le 15$. For a Debye relaxation ($\tilde{c}'' = x/(1 + x^2)$, $x = \omega/\omega_T$, $\beta \equiv 1$) the case is rather trivial and we get analytically $F \equiv 1$.

In summary, the average temperature fluctuation $\overline{\Delta T^2}$ of a cooperatively rearranging region CRR is equal to the temperature dispersion δT^2 from a Gaussian approximation of the isochronal $C''(T)$ curve (eq 4) if

(i) the temperature fluctuation is obtained from the fluctuation dissipation theorem FDT,

(ii) at least the central part of the equilibrium $c''(T)$ curve can reasonably be approximated by a Gauss function, and

(iii) the trace of the c'' maximum temperatures T_ω for different ω in a $T_\omega(\ln \omega)$ plot is approximately linear in the interval $T_\omega - \delta T ... T_\omega + \delta T$.

The difficulties with the c_p/c_V conversion are not touched by this calculation.

References and Notes

(1) Adam, G.; Gibbs, J. H. *J. Chem. Phys.* **1965**, *43*, 139.
(2) Schmidt-Rohr, K.; Spiess, H. W. *Phys. Rev. Lett.* **1991**, *66*, 3020.

(3) Heuer, A.; Wilhelm, M.; Zimmermann, H.; Spiess, H. W. *Phys. Rev. Lett.* **1995**, *75*, 2851.
(4) Tracht, U.; Wilhelm, M.; Heuer, A.; Feng, H.; Schmidt-Rohr, K.; Spiess, H. W. *Phys. Rev. Lett.* **1998**, *81*, 2727.
(5) Russel, E.; Israeloff, N.; Walther, L.; Gomariz, H. *Phys. Rev. Lett.* **1998**, *81*, 1461.
(6) Donth, E. *J. Non-Cryst. Solids* **1982**, *53*, 325.
(7) Hempel, E.; Kahle, S.; Unger, R.; Donth, E. *Thermochim. Acta* **1999**, *329*, 97.
(8) Arndt, M.; Stannarius, R.; Groothues, H.; Hempel, E.; Kremer, F. *Phys. Rev. Lett.* **1997**, *79*, 2077.
(9) Pissis, P.; Kyritsis, A.; Daoukaki, D.; Barut, G.; Pelster, R.; Nimtz, G. *J. Phys.: Condens. Matter* **1998**, *10*, 6205.
(10) Schick, C.; Donth, E. *Phys. Scr.* **1991**, 43, 423.
(11) Hu, H.; Carson, G.; Granick, S. *Phys. Rev. Lett.* 1991, *66*, 2758.
(12) Inoue, T.; Cicerone, M.; Ediger, M. *Macromolecules* **1995**, *28*, 3425.
(13) Fujara, F.; Geil, B.; Sillescu, H.; Fleischer, G. *Z. Phys. B* **1992**, *88*, 195.
(14) Fischer, E. *Physica A* **1993**, *201*, 183.
(15) Fischer, E. W.; Donth, E.; Steffen, W. *Phys. Rev. Lett.* **1992**, *68*, 2344.
(16) Debye, P.; Bueche, A. *J. Appl. Phys.* **1949**, *20*, 518.
(17) Moynihan, C. T.; Schroeder, J. *J. Non-Cryst. Solids* **1993**, *160*, 52.
(18) Schiener, B.; Böhmer, R.; Loidl, A.; Camberlin, R. *Science* **1996**, *274*, 752.
(19) Mel'cuk, A.; Ramos, R.; Gould, H.; Klein, W.; Mountain, R. *Phys. Rev. Lett.* **1995**, *75*, 2522.
(20) Horbach, J.; Kob, W.; Binder, K.; Angell, C. A. *Phys. Rev. E* **1996**, *54*, R5897.
(21) Sillescu, H. *J. Non-Cryst. Solids* **1999**, *243*, 81.
(22) Donth, E. *Acta Polym.* **1979**, *30*, 481.
(23) Richert, R. *Chem. Phys. Lett.* **1993**, *216*, 223.
(24) Johari, G. P.; Pathmanathan, K. *Phys. Chem. Glasses* **1988**, *29*, 219. Johari, G. P.; Hallbrucker, A.; Mayer, E. *J. Polym. Sci. Part B: Polym. Phys.* **1988**, *26*, 1923.
(25) Zorn, R.; Arbe, A.; Colmenero, J.; Frick, B.; Richter, D.; Buchenau, U. *Phys. Rev. E* **1995**, *52*, 781.
(26) Arbe, A.; Richter, D.; Colmenero, J.; Farago, B. *Phys. Rev. E* **1996**, *54*, 3853.
(27) Arbe, A.; Colmenero, J.; Monkenbusch, M.; Richter, D. *Phys. Rev. Lett.* **1998**, *81*, 590.
(28) Donth, E. *Acta Polym.* **1999**, *50*, 240.
(29) Leheny, R. L.; Menon, N.; Nagel, S. R.; Price, D. L.; Suzuya, K.; Thiyagarajan, P. *J. Chem. Phys.* **1996**, *195*, 7783.
(30) Donth, E. *J. Polym. Sci. Part B: Polym. Phys.* **1996**, *34*, 2881.
(31) Birge, N. O.; Nagel, S. R. *Phys. Rev. Lett.* **1985**, *54*, 2674.
(32) Korus, J.; Beiner, M.; Busse, K.; Kahle, S.; Unger, R.; Donth, E. *Thermochim. Acta* **1997**, *304/305*, 99.
(33) Korus, J.; Hempel, E.; Beiner, M.; Kahle, S.; Donth, E. *Acta Polym.* **1997**, *48*, 369.
(34) Donth, E. *Glasübergang*; Akademie-Verlag: Berlin, 1981.
(35) Donth, E. *Relaxation and Thermodynamics in Polymers. Glass Transition*: Akademie-Verlag: Berlin, 1992.
(36) Donth E. *Phys. Rev. E*, submitted.
(37) von Laue, M. *Phys. Z.* **1917**, *18*, 542.
(38) Landau, L. D.; Lifshitz, E. M. *Statistical Physics*, 3rd ed.; Pergamon Press: Oxford, **1980**; Part 1, Chapter XII, pp 112 and 114.
(39) Angell, C. A. *J. Non-Cryst. Solids* **1991**, *131*, 13.
(40) O'Reilly, J. M. *J. Polym. Sci.* **1962**, *57*, 429; *J. Appl. Phys.* **1977**, *48*, 4043; *J. Polym. Symp.* **1978**, 165.
(41) Narayanaswamy, O. S. *J. Am. Ceram. Soc.* **1971**, *54*, 491.
(42) DeBolt, M. A.; Easteal, A. J.; Macedo, P. B.; Moynihan, C. T. *J. Am. Ceram. Soc*. **1976**, *59*, 16.
(43) Kahle, S.; Hempel, E.; Beiner, M.; Unger, R.; Schröter, K.; Donth, E. *J. Mol. Struct.* **1999**, *479*, 149.
(44) Schneider, K.; Schönhals, A.; Donth, E. *Acta Polym.* **1981**, *32*, 471.
(45) Hensel, A., Dissertation, Universität Rostock, 1998; Hensel, A.; Schick, C. *J. Non-Cryst. Solids* **1998**, *235*−*237*, 510.
(46) Privalko, V. P. *J. Phys. Chem.* **1980**, *84*, 3307. Wunderlich, B.; Jones, L. D. *J. Macromol. Sci., Phys.* **1969**, *B3*, 67.
(47) Beiner, M.; Kahle, S.; Hempel, E.; Schröter, K.; Donth, E. *Europhys. Lett.* **1998**, *44*, 321.
(48) Götze, W.; Sjögren, L. *Rep. Prog. Phys.* **1992**, *55*, 241.
(49) Kahle, S.; Korus, J.; Hempel, E.; Unger, R.; Höring, S.; Schröter, K.; Donth, E. *Macromolecules* **1997**, *30*, 7214.
(50) Kahle, S.; Schröter, K.; Hempel, E.; Donth, E. *J. Chem. Phys.* **1999**, *111*, 6462.
(51) Angell, C. A.; Sichina, W. *Ann. N.Y. Acad. Sci.* **1976**, *279*, 53.
(52) Moynihan, C. T.; Easteal, A. L.; Tran, D. C.; Wilder, J. A.; Donovan, E. P. *J. Am. Ceram. Soc.* **1976**, *59*, 137.
(53) Saurina, J.; Mora, M. T.; Clavaguera, N. *J. Therm. Anal.* **1998**, *52*, 845.
(54) Coenen, M. *Glastechn. Ber*. **1977**, *50*, 115. The silicate glasses are the numbers 2, 5, 6, 13, 14, and 15 in Coenen's publication. The results are from an average over all six glasses.
(55) Mizukami, M.; Fujimori, H.; Masaharu, O. *Solid State Commun.* **1996**, *100*, 83.
(56) Beiner, M.; et al. To be published.
(57) Böhmer, R.; Ngai, K. L.; Angell, C. A.; Plazek, D. J. *J. Chem. Phys.* **1993**, *99*, 4201.
(58) Note added at proof: An analytical solution based on the Kramers Kronig relation for the modulus gives $F = 1$ for all shapes of $c^*(\omega)$. Lellinger, D. Private communication, 2000.